RSC Advances

ROYAL SOCIETY OF CHEMISTRY

www.rsc.org/advances

Removal of Rhodamine B from wastewater by modified *Volvariella volvacea*: batch and column study

Qiao Li, Xia Tang, Yuanyuan Sun, Yifan Wang, Yunchuan Long, Juan Jiang, Heng Xu*[1]

Key Laboratory of Bio-resources and Eco-environment (Ministry of Education), College of Life Science, Sichuan University, Chengdu, Sichuan 610064, China.

[1] *Corresponding author. Tel: +86 28 85414644; Fax: +86 28 85418262
E-mail address: xuheng64@sina.com(H. Xu).

Abstract:

This study investigated the biosorption of Rhodamine B (a carcinogenic dye) onto *Volvariella volvacea* in batch and bed column experiments. Hexadecyltrimethylammonium bromide modified *V. volvacea* (HMV) showed best performance in removing Rhodamine B with a biosorption capacity of 33.51mg g^{-1}. Langmuir isotherm and pseudo-second-order kinetic models described well with the experimental data from batch mode. Initial concentration, flow rate, and bed height significantly influenced the dye removal in the continuous column process. Bohart-Adams, Thomas and Yoon-Nelson models successfully fitted with breakthrough curves obtained under varying experimental conditions. The applicability of HMV was tested using simulated industrial wastewater, and the results confirmed that several dyes and other contaminants could be effectively removed by HMV. *V. volvacea* is an efficient and economical biosorbent for the removal of dye from wastewater.

Key words: Biosorption; *Volvariella volvacea*; Fixed bed column; Dye; Modification.

1. Introduction

Many industries such as paper and pulp, cosmetics, paint and pigments, plastics, leather tanning and textile industries give rise to a large amount of coloured effluent and substantial quantity of cations and anions (Anandkumar and Mandal, 2011). According to statistics, there are 744 tones waste water generated when 1 ton dyes are manufactured, the average loss rate of around 20% dyes in the production process of dyeing and printing process, among them about half are discharged into the environment (Ozmen et al., 2007). Besides dyes, such effluents contain a great many of other contaminants, for instance, acids or alkalis, salts, dissolved and suspended solids, and other compounds, which are of great toxic (Maurya et al., 2006). The dyes are adsorbed and reflected of sunlight entering the water (Fu and Viraraghavan, 2002; O'Mahony et al., 2002). The dye components are barely degraded by physical, chemical methods and degradation becomes extremely untoward as the textile dyes

are frequently being replaced with modern dyes, which resistant to chemical, photochemical, and biological degradation (Won et al., 2004). Rhodamine B (RB), a synthetically prepared carcinogenic xanthine dye is widely used for paper printing, pot-metal glass, textile dyeing, fireworks and crackers, leather and paint industries, what's more, it is also applied for cell fluorescent stain in the laboratory (Das et al., 2008). It brings serious pollution and great damage when it let out into our environment and consumed by human beings and animals, eventually causes irritation to the skin, eyes and respiratory tract because of its carcinogenicity, reproductive and developmental toxicity, neurotoxicity and chronic toxicity (Inbaraj et al., 2006; Kadirvelu et al., 2005). Therefore, the treatment of dye-contaminated effluents is of significant environmental and commercial importance (Akar et al., 2009).

A series of chemical, physical and biological measures, which remove dyes from effluents have developed such as decolourisation, chemical coagulation, chemical oxidation, electrolytic process, ion-exchange membrane separation, aerobic and anaerobic microbial degradation (Lei et al., 2014). Among these removal technologies, adsorption is supposed to be the most popular physicochemical due to the ease of operation and comparable low cost of application. Low cost materials such as brown macroalga (Kousha et al., 2012), straw (Zhang et al., 2012), bentonites (Koyuncu et al., 2011), Clays (Sarma et al., 2011) and mushroom (Arica and Bayramoglu, 2007) have been reported to be utilized as biosorbent for the efficient removal of dyes from aqueous solution.

The column type with continuous flow operations is commonly used for gas and liquid pollution control (Auta and Hameed, 2014). Thus, fixed-bed adsorption system can be applied for dealing with effluent and which can create room for treatment of large volume of effluent fluid with less monitoring requirement; moreover, it is simple to operate and can be easily scaled up (Singh et al., 2012; Yaghmaeian et al., 2014). A survey of the latest literature shows that diverse fungal organisms are capable of decolorizing a wide range of dyes and much work have been performed on species of

fungal for the removal of different dyes from wastewater (Nguyen and Juang, 2013). The edible straw mushroom, *Volvariella volvacea*, is one of the most extensively cultivated mushrooms in China, ranking the second or the third position in terms of annual edible mushroom industrial production worldwide (Wang et al., 2008). Furthermore, *V. volvacea* was first used to remove dyes in fixed bed column.

The objective of the present study is to research the potential of modified *V. volvacea* for RB removal in batch and continuous fixed bed systems. The surface characterization of raw and hexadecyltrimethylammonium bromide-modified *V. volvacea* (HMV) were analyzed using Scanning Electron Microscope (SEM) and Fourier Transform Infrared Spectrometry (FTIR). The operational parameters such as adsorbent dosage, pH, and initial concentration were investigated. Adsorption isotherm models and kinetics models were studied in batch experiment. The effect of initial dye concentration, flow rate, and bed height on biosorption capacity were investigated in fixed bed. Three models, Bohart–Adams, Thomas, and Yoon–Nelson models, were applied to analyze the breakthrough curves. The applicability of the adsorbent to treat RB contaminated wastewater, in a fixed bed column, was examined by using simulated industrial wastewater.

2. Materials and methods

2.1 Adsorbate

Cationic dye, namely Rhodamine B (C.I. = 45170), was selected as the representative cationic dye. All reagents used in this study were of analytical grade chemicals and purchased from KeLong, Chemical Reagent Factory, Chengdu, China. A stock solution of RB (1000 mg L^{-1}) was prepared by dissolving appropriate quantity of Rhodamine B in ultrapure water and the required initial concentrations (50, 100, 150 mg L^{-1}) were obtained when needed by suitably diluting the stock solution with deionized water. Before mixing the adsorbent, the pH values were adjusted using HCl (0.1, 1 M) or NaOH (0.1, 1 M) and measured by pH meter.

Simulated industrial wastewater containing various constituents was prepared in the laboratory, which were completely mixed in the appropriate amount of tap water. The SIW composition was as follows: Malachite green (MG, 50 mg L^{-1}), RB (50 mg L^{-1}), Neutral Red (NR, 50 mg L^{-1}), Crystal violet (CV, 50 mg L^{-1}), NaH_2PO_4 (0.3 mmol L^{-1}), NaCl (0.5 mmol L^{-1}), $NaSO_4$ (0.2mmol L^{-1}), $NaHCO_3$ (0.4 mmol L^{-1})

2.2 Adsorbent

Fresh *V. volvacea* was obtained from a nearby mushroom production site of Chengdu, China. It was then washed thoroughly with distilled water and dried at 323± 1 K for 3 d in an oven drier. The oven-dried sorbent was ground to a fine powder with a pulverizing mill (Joyoung, JYLC012) and sieved to desired mesh size (40 – 60 mesh) then stored in a plastic bottle for further use.

2.3 Pretreatment of adsorbent

2.3.1 Methylation of amines

The modification of amino functional groups was done by shaking 1 g of the dried biomass in an Erlenmeyers flask containing 20 mL of pure formaldehyde (HCHO) and 40 mL of formic acid (HCOOH) for 12 h with agitation speed of 145 rpm at 30℃. This treatment resulted in methylation of amine. The general scheme for this reaction is:

$$RCH_2NH_2 \xrightarrow{HCHO,HCOOH} RCH_2N(CH_3)_2 + CO_2 + H_2O \quad (1)$$

After reaction, the modified biomass washed several times with ultrapure water and dried at 323±1 K for 2 d.

2.3.2 Hexadecyltrimethylammonium bromide treatment

The amount of hexadecyltrimethylammonium bromide (HDTMABr) (0.24 g) was

dissolved in 50 mL deionized water and 1 g of powdered raw biosorbents was added and agitated with a magnetic stirrer for 12 h at 145 rpm. Following the mixing period, the resulting biomass was centrifuged at 3000 rpm for 5 min, washed, centrifuged, dried, ground, and sieved following the above-mentioned methods for the later experiments.

2.3.3 Sodium chloride treatment

Fifty milliliters of 1000 mg L^{-1} NaCl was added to 1 g of crushed mealy biomass and the reaction mixture was shaken in a shaker incubator (SUKUN, SKY211B) for 12 h with agitation speed of 145 rpm at 30℃.

2.3.4 Sulfuric acid treatment

The modification experiment was carried out in a 150 mL stoppered three-neck round bottom flask with adding 50 mL of 0.05 M H_2SO_4 and 1 g of adsorbents. The flask was placed at a shaker with a shaking of 145 rpm at 30℃ for 12h.

2.4 Characterization of adsorbent

The surface morphology features of unprocessed and modified biosorbent were observed by Scanning Electron Microscopy (SEM) (JSM-5900LV, Japan). A Fourier Transform Infrared spectrometer (FTIR) (NEXUS-650, America) was used to analyse the dominating functional groups on the adsorbent surface. The pH at the point of zero charge (pH_{PZC}) of the raw biomass, namely the pH value required to give zero net surface charge, was determined by mass titration (Lei et al., 2014).

2.5 Batch experiments

A series of experiments were conducted in 250 mL Borosil conical flasks containing 50 mL of dye solution. A weighed amount of HDTMABr modified *V. volvacea* (HMV) was added to RB solutions. The mixtures were shaken on a constant

temperature breeding shaker (SUKUN, SKY-211B) at 145 rpm for 12 h. The effect of pH (2.0–6.0), contact time (0-330 min), initial dye concentration (50–250 mg L^{-1}), sorbent dose (1-5g L^{-1}), and adsorption temperature (20, 30, 40℃) were evaluated in order to find out the optimum conditions for the dye biosorption. All adsorption experiments were conducted in duplicate, control experiments were also performed without the addition of adsorbent to confirm that the adsorption of the dye onto Erlenmeyers flasks was trivial. After biosorption, the supernatant of dye solution was separated by centrifuge (Thermo) at 3000 rpm for 5min, and then the filtrate was analyzed for the residual RB concentration using UV/vis spectrophotometer at the maximum absorption wavelength (λ_{max} = 553 nm) of RB.

2.6 Fixed bed column studies

Fixed bed biosorption studies were conducted to evaluate dynamic behavior for RB removal on HMV in a glass column with an internal diameter of 1.5 cm and 10 cm in length. HMV with designed height was packed in the glass column between two supporting layers of glass wool. A layer of glass beads was placed at the top to provide a consistent inlet flow (Long et al., 2014). All column studies were performed by pumping dye solution in a down-flow mode using a constant flow pump at room temperature of 30℃ and optimum pH 5. The impact of HMV dosages (0.5, 1 and 1.5 g), flow rate (0.5, 2 and 3.5 mL min^{-1}) and dye solution with different initial RB concentrations (50, 100, 150 mg L^{-1}) on biosorption process in fixed bed column was investigated at the same time.

2.7 Treatment of simulated industrial wastewater in fixed bed column

The applicability of fixed-bed in treating industrial wastewater was tested through simulating industrial wastewater. The simulated industrial wastewater adjusted to pH 5.0 was treated in the column packed with HMV at optimum bed height and flow rate till the biosorbent was saturated. The treated samples collected from the exit were

analyzed for the concentrations of Malachite green, Rhodamine B, Neutral red, Crystal violet.

2.8 Fixed bed column biosorption process analysis

Several experimental parameters, which were calculated for fixed-bed dye sorption process, are of critical importance in the continuous column. Fixed-bed capacity, q_c (mg), is equal to the area under the plot from the integral of adsorbed concentrations expressed as C_{ad} ($C_{ad} = C_0\text{-}C_t$) mg L^{-1} for a given time t (min) and is calculated as follows (Auta and Hameed, 2014):

$$q_c = \frac{Q \,.\, A}{1000} = \frac{Q}{1000} \int_0^t C_{ad} \,.\, dt \quad (2)$$

where Q and A are the effluent flow rate (mL min^{-1}) and the area under the breakthrough curve, respectively, t is the total flow time (min).

The total dye removal (R%) can be calculated from the ratio of fixed-bed capacity (q_c) to the quality of the dye sent to the column (m) as:

$$R\% = \frac{q_c}{m} \times 100 \quad (3)$$

The equilibrium uptake q, the weight of RB adsorbed per unit dry weight of adsorbent can be evaluated using (Aksu and Gönen, 2004; Malkoc et al., 2006):

$$q = \frac{q_c}{X} \quad (4)$$

where X (g) is the mass of the total biosorbent in the column.

2.9 Kinetic models of fixed bed column adsorption

These three modeling of breakthrough curves have been tested in the present study: Bohart-Adams, Thomas, and Yoon-Nelson models. Bohart-Adams model, which is

based on the surface reaction theory, is one of the most common equation used to describe the initial part of breakthrough curves (Quintelas et al., 2013). This model assumes that equilibrium is not instantaneous and have rectangular shape isotherm. The Thomas model (Thomas, 1948) was frequently applied for describing the column performance and predict the breakthrough curve of the sorption process in a packed bed reactor. Yoon-Nelson established a model to depict the breakthrough behavior of absorbate on adsorbent so its kinetic model stands on the precondition that the rate of decrease in the probability of sorption of each adsorbate molecule is proportional to the probability of adsorbent (Long et al., 2014). All the above-mentioned kinetic models are represented in Table 1.

3. Results and discussion

3.1 Effect of modification

Both native and modified *V. volvacea* have been used to remove the hazardous pollutant from wastewater. Fig.1 shows the uptake of RB by native and modified *V. volvacea*. The biosorption capacity of the native biosorbent for RB was 8.17 mg g^{-1} dry biomass. The sorption capacities of the acid, NaCl and HDTMABr pretreated biomass were increased about 1.07-, 1.12- and 4.1-fold compared to the control group, respectively; whereas a decrease in adsorption capacity of the formaldehyde and formic acid treated adsorbent was observed with 1.08-fold.

HDTMABr-modified *V. volvacea* (HMV) showed the best performance with a biosorption capacity of 33.51 mg g^{-1}. The surface property of HMV was characterized by irregular and porous after modification with HDTMABr (Fig.2); moreover, functional groups on the mushroom surface were increased via the denaturation or dissolution of biopolymers (Fig.3), thus enhance biosorption capacity (Koyuncu et al., 2011). Higher adsorption efficiency of NaCl-modified biomass could be due to the dissociation and the increasing swell of some components. For sulfuric acid, acid treatment changes the regular pattern of the adsorbent structure accompanied by

211 partial distortion as H^+ ions replace some of the exchangeable cations on the
212 adsorbent surface (Sarma et al., 2011). On the other hand, the formaldehyde and
213 formic acid treated biomass showed the lowest biosorption capacity, which against
214 with the result of an increase of dye adsorption (Kousha et al., 2012), could account
215 for the disadvantage of the methylation of amino functional groups boned onto the
216 biomass surfaces.

217 ***3.2 Surface characterization of adsorbent***

218 The morphological structure of the raw and HDTMABr modified biosorbents
219 presented in Fig.2 revealed by SEM (at magnification 5000×) showed that the fungal
220 biomass was characterized by an irregular and porous surface. The porous surface
221 structure of the biosorbent should be the reason for an increase specific surface area.
222 In addition, these irregulars and pores decrease the mass transfer resistance and
223 facilitate the diffusion of dye molecules, thus enhance biosorption efficiency (Arica
224 and Bayramoglu, 2007).

225 The FTIR spectra of unmodified *V. volvacea* and HMV are shown in Fig.3. The
226 peak at 3429 cm^{-1} indicated the -NH stretching vibrations superimposed on the side of
227 –OH (Charumathi and Das, 2012); The peak at 2921cm^{-1} corresponding to stretching
228 of the C-H bonds of the methyl and methylene groups (Akar et al., 2009); The peak at
229 1647cm^{-1} represents $–NH_2$ group (Long et al., 2014); The peak at 1378 and 1070 cm^{-1}
230 corresponding to the C–H bending ($–CH_3$) and C–OH stretching vibrations,
231 respectively (Quintelas et al., 2013). The band at 522cm^{-1} represents C-N-C
232 scissoring that is only found in protein structures (Akar et al., 2009).

233 ***3.3 Effect of biosorbent dose on biosorption of RB***

234 The effects of absorbent dose were tested by using different quantities of sorbent
235 and these results are presented in Fig. 4. It showed that the percentage biosorption
236 yield increased with increasing in the adsorbent amounts. At equilibrium time of 5 h,

the removal percentage increased from 24.47% to 86.33% when the biomass concentration increased from 1 to 5 g L^{-1}. The increase of RB removal with biomass dose may be owing to the increase surface areas of biosorbent and availability of more possible biosorption sites. Similar observation was previously reported by other researchers (Tian et al., 2011). A further increase in biomass concentration over 5 g L^{-1} did not bring about a significant improvement in biosorption at adsorption equilibriums due to saturation of the adsorbent surface areas with dye molecules. Therefore, the optimum biosorbent concentration was selected as 5 g L^{-1} for economic considerations.

3.4 Effect of solution pH on RB biosorption

The effect of initial solution pH on the percent removal of RB by HMV at equilibrium conditions was studied at total six pH values among 2-8 for the initial dye concentration of 100 mg L^{-1} at 30 ℃. As shown in Fig.5, the adsorption percent increased from 55.2 to 68.68 while initial solution pH increased 2 to 5 and decreased from 68.68 to 41.87 in the pH range of 5 to 8. The optimum initial solution pH was 5.0 and it was used in following studies.

RB, an aromatic amino acid, it changes its basicity or acidity with the change of pH. When below pH 4.2, the RB molecules are positive charged and the carboxylic group is unionized; while at a higher pH, i.e. above 4.2, the RB is net negatively charged (Maurya et al., 2006). In addition, the point of zero charge of the adsorbent, pHpzc, was around 6.28. When the solution pH was below the pH_{PZC}, the surface of HMV was charged positively. Nevertheless, when the pH was above the pHpzc, the surface was charged negatively (Lei et al., 2014). Therefore, when the pH higher than 4.2 but below 6.28, the surface of HMV was positively charged, while the RB ions contained negative charges, hence the high electrostatic attraction led to higher RB biosorption.

3.5 Effect of contact time

The contact time was assessed as an important parameter affecting the adsorption capacity of adsorbent. Fig.6 presents the effect of contact time on the removal of RB dyes by HMV for various initial dye concentrations. The results showed that adsorption capacity of biosorbent at different initial concentrations increased rapidly at the starting stage of biosorption process and, thereafter, the adsorption rate decreased gradually and then biosorption reached equilibrium after some time. In the start, the rapid adsorption of dye may be attributed to the instantaneous utilization of the most readily available active sites on the surface of biosorbent (Dawood and Sen, 2012). After some period of contact time, the biosorption began to slow down due to the saturation of the available binding sites on the adsorbent surface (Sadaf and Bhatti, 2013). Furthermore, an increase in initial dye concentration led to increase in the biosorption uptake of dye, so was the equilibrium time. This is so because a higher initial concentration increased the number of collisions between dye molecules and biosorbents and enhanced the driving force between the solution and solid phases (Wang et al., 2010).

3.6 Effect of initial concentration on RB biosorption

Profiles for RB uptake by HMV at different initial concentrations are shown in Fig. 7. The biosorption capacity of the modified adsorbent increased from 24.2 to 46.87 mg g^{-1} with increasing of the initial concentration of dye in the biosorption medium, although the removal percentage decreased from 96.8 to 37.5. The reduction of the removal percentage may be attributed to abundant active sites on HMV which outstripped the scanty molecules of adsorbates in low concentrations, and the limited active sites were saturation for superfluous adsorbate molecules at higher concentrations (Zhou et al., 2011). The concentration difference provides the prerequisite driving force to conquer the resistances to the mass transfer of RB between the liquid phase and the solid phases, and thus greatly enhances the interaction between dye molecule and biosorbent, which may account for the improvement of the adsorption capacity (Zhang et al., 2012).

3.7 Biosorption isotherms

Adsorption isotherms provide momentous information that reveals the equilibrium relationship between the adsorbate concentration in the liquid phase and the solid phase at a constant temperature. Three isotherm models, Langmuir, Freundlich and Temkin equations were chosen to describe the equilibrium characteristics of this biosorption study (Table 2). The results are presented in Table 3 and isotherm plots for RB adsorption on HMV at 30 °C is showed in Fig. 8. As seen from Table 3, the regression coefficients (R^2) of Langmuir model were more than 0.99 under specific conditions, which were higher than the R^2 of Freundlich model (0.9745-0.986) and Temkin model (0.9174-0.9295). Moreover, it can be seen from Fig.8 that the experimental data fitted Langmuir isotherm better than the other two isotherms. This indicated that Langmuir model was more suitable for the sorption process of HMV in the present study, indicating monolayer adsorption of RB occurred on a heterogeneous adsorbent surface. It is also can be seen from Table 3 that the maximum monolayer biosorption capacity (q_m) of HMV for RB were 61.35 $mg.g^{-1}$, 68.49 $mg.g^{-1}$, 94.34 $mg.g^{-1}$ at 20℃, 30℃, 40℃, respectively. Moreover, the value of k_L was in the range of 0-1 which confirms the favorable uptake of RB.

3.8 Kinetics of RB biosorption on HMV

In order to investigate the adsorption mechanism and characteristics of RB dye onto HMV, two models (pseudo-first-order and pseudo-second-order models) were used to test the experimental data.

The pseudo-first-order equation is generally expressed as follows (Mahmoud et al., 2012):

$$\log(q_e - q_t) = \log q_e - \frac{k_1}{2.303} t \quad (5)$$

The pseudo-second-order equation based on adsorption equilibrium capacity could

be represented as (Dawood and Sen, 2012; Gupta et al., 2011):

$$\frac{t}{q_t} = \frac{1}{k_2 q_e^2} + \frac{t}{q_e} \quad (6)$$

where q_e and q_t (mg g^{-1}), are the amount of dye adsorbed at equilibrium and at any time *t* (min) per unit weight of adsorbent, respectively; k_1 (min^{-1}) and k_2(g/mg min), which are calculated from the slopes of $\log(q_e - q_t)$ versus *t* and $\frac{t}{q_t}$ versus *t*, are rate constants of pseudo-first-order and pseudo-second-order adsorption (Fig. not shown), respectively.

The values of parameters and R^2 are shown in Table 4. With higher R^2 value, pseudo-second-order model was more fitted the biosorption data than the pseudo-first-order model. Moreover, its calculated adsorption capacity is closely fitted with the experimental data. Therefore, the present adsorption system follows predominantly the pseudo-second-order kinetics model. A similar result for the treatment of dye effluent has also been reported in other work (Bouzid et al., 2015; Elkady et al., 2011).

3.9 Thermodynamics of biosorption

Thermodynamic parameter related to the adsorption process, the free energy change (ΔG^0, kJ mol^{-1}), enthalpy change (ΔH^0, kJ mol^{-1}) and entropy change (ΔS^0, kJ mol^{-1}) were calculated using the following equations:

$$\Delta G^0 = -RT \ln K_0 \quad (7)$$

$$\Delta G^0 = \Delta H^0 - T\Delta S \quad (8)$$

where R is the universal gas constant (8.314 J/Kmol), T the absolute temperature (K) and K_0 the distribution coefficient expressed as $K_0 = C_e$ (adsorbent)/C_e (solution). The values of thermodynamic parameters are shown in Table 5. The values

of free energy changes (ΔG^0) were negative, indicating the feasibility and spontaneous nature of adsorption process. The positive value of ΔS^0 for HMV indicates the increased randomness at the solid/solution interface during the RB adsorbed onto the active sites of biosorbent (Gupta et al., 2011), suggests good affinity of the dye towards the adsorbent and significant changes occur in the internal structure of the biosorbents through the biosorption (Akar et al., 2009). Further, the positive ΔH^0 value confirmed that biosorption of RB dye by HMV is an endothermic process.

3.10 Fixed bed adsorption column study

3.10.1 Effect of initial concentration

The effect of initial influent stream at 2 mL min^{-1} to a constant bed height of 4cm had its concentration variations of 50, 100 and 150 mg L^{-1}. Table 6 summarizes the values of the experimental breakthrough parameters. The results are presented in Fig.9. It can be seen from the Table 6 that the breakthrough time and exhaustion time were inversely proportional to the influent RB dye concentration. In addition, at lower initial RB dye concentrations, the breakthrough curves were prolonged, while at a higher concentration, shorter stretch of the breakthrough curves signifying smaller dye solution treatment capability. This could be explained by the fact that at the lower concentration, smaller mass transfer caused a treatment of more volume of RB solution during the adsorption process (Singh et al., 2012). Moreover, the results demonstrated that the biosorption capacity increased with solute concentration of 50, 100 and 150 mg L^{-1} corresponding to 18.41, 21.42 and 28.09 mg g^{-1}, respectively. This trend indicated that the higher influent concentration could saturate the biosorbent more quickly. Similar trend has been reported for the biosorption of Drimarine Black CL-B dye by using peanut husk (Sadaf and Bhatti, 2013).

3.10.2 Effect of influent flow rate

Flow rate plays a significant role in the determination of contact time of the adsorbate with the adsorbent in the continuous treatment of industrial wastewater. The effect of different flow rates (0.5, 2, 3.5 mL min^{-1}) on the biosorption of RB dye using HMV at a constant bed height (4 cm) and 100 mg L^{-1} inlet RB concentration in column was investigated. The breakthrough curves at varying flow rates illustrated in Fig.10 indicate that the saturation time and breakthrough time decrease significantly at higher flow rates. This might be the enhancement in amount of dye adsorbed onto unit bed height (mass transfer zone) at higher flow rate that caused the reduction in time needed to saturate (Noreen et al., 2013). In this study, the biosorption capacity of RB dye decreased by the increase in flow rate of influent stream, which might be due to transitory residence time of dye molecules in the column at a high flow rate, and therefore, it cannot lead to the equilibrium after the solute left the column of the adsorption process (Charumathi and Das, 2012).

3.10.3 Effect of bed height

The effect of a variation of bed height from 2 to 6 cm filled with modified sorbent was investigated at constant flow rate and inlet RB concentration of 2 mL min^{-1} and 100 mg L^{-1}, respectively. The breakthrough profiles of RB biosorption at three different bed heights were presented in Fig.11. It was found that the breakthrough time was 11, 54, and 72 min for 2, 4, 6 cm bed heights and the complete bed exhaustion time were 106, 160, and 175 min, respectively. This may be explained on the increase in the amount of biosorbent in the column which translates to increase in binding sites (Vieira et al., 2014). In this study, the sorption capacity was slightly decreased with increasing in bed height. This result was in argument with the conclusions of other researchers who found a positive correlation between the adsorption capacity and bed height (Singh et al., 2012). They attributed the improvement of sorption capacity to sufficient contact time between dye molecules and available adsorbent. The volume of treated effluent increased at a higher bed height because of a longer residence period of dye molecules that more biosorbent

provided.

3.11 Modeling of the breakthrough curves

Bohart-Adams adsorption model was used for the description of the initial part of the breakthrough curves of RB biosorption, and respective values of N_0, and k_{BA} were calculated and summarized in Table 7 coupled with the correlation coefficients (R^2). The values of correlation coefficients were found to be above 0.9738 at all conditions. It is seen from the Table 7 that the saturation concentration (N_0) of fixed-bed increased with increasing initial RB concentration, but decreased with increasing bed height and flow rate. In addition, kinetic constant (k_{BA}) decreased with increasing initial RB concentration and bed height; however, it increased with increasing flow rate. Results indicate that the overall system kinetics were dominated by external mass transfer in the initial part of sorption process in the fixed bed (Sajab et al., 2014). Therefore, bed height should be higher while flow rate should be lower for better saturation concentration (N_0) and lower kinetic constant (k_{BA}) of the column.

Thomas and Yoon-Nelson models fitted quite well to the breakthrough curves (R^2>0.9916) obtained from the adsorption of RB dye by the HMV-packed column under various experimental conditions. The Thomas rate constant, k_T, was higher at higher flow rate of dye solution passing through column, shorter bed height and lower initial dye concentration. The maximum solid phase concentration (q_0) increased significantly with increasing inlet RB dye concentration and opposite trend was seen in case of bed height and flow rate. Usually, the rate constant (k_Y) of Yoon-Nelson model increased with increasing inlet dye concentration and higher flow rate; and yet it reduced with increasing bed height. However, the value of τ, the time required for 50% breakthrough, increased with increasing bed height; nevertheless, it reduced with increase in both inlet dye concentration and flow rate. Similar result was reported for the adsorption of Reactive Black by granular activated carbon (Yaghmaeian et al., 2014).

3.12 Applicability of column in treating simulated industrial wastewater

Since the ultimate purpose of the dye adsorption technology is removal of dye molecules from the effluents that often contain several dye molecules, anion and cation simultaneously, adsorption experiments were conducted with simulated industrial wastewater. Thomas model was applied to analyze the experimental data of dye removal from simulated industrial wastewater, and the values characteristic parameters are listed in Table 8. The correlation coefficients (R^2) values were found to be lower compared to single solute system. The results showed that NR molecules could be prior removed from wastewater in the presence of other dye molecules (RB, CV, MG) in a multi-dye system. Nonetheless, for the column packed with modified biosorbent treated with simulated industrial wastewater, the removal of each dye molecules is completely affected, the individual adsorption capacity (q_0) of bed was much lower compared to single solution system, while the total adsorption capacity was 41.52 mg g^{-1}, which was significantly increased. This may be explained that there still remained several active sites which were selectively combined with other dye molecules when absorbent has reached saturation of one kind of dye in multi-dye system, as a result, the overall adsorption capacity is higher than in single-dye system. However, some researchers presented different results (Singh et al., 2012, Vimala et al., 2011). The present study demonstrates that HMV-packed column is capable of removing multi-dye from industrial wastewater.

4. Conclusions

HDTMABr modified *V. volvacea* was successfully prepared and showed best performance in removing RB with a biosorption capacity of 33.51mg g^{-1}. SEM and FTIR have been used to analyze the surface characterization of *V. volvacea*. Biosorption activities were primarily on the monolayer surface with high adsorbate-adsorbent interaction as exhibited by the isotherms models studies which were in accordance with fitness Langmuir and Freundlich, respectively. RB adsorption performance of the column packed with HMV was found to be

449 significantly depended on influent dye concentration, flow rate, and bed height.
450 Bohart-Adams, Thomas and Yoon-Nelson models were applied to analyze the column
451 experimental data which successfully predicted breakthrough curves acquired under
452 different experimental conditions. The *V. volvacea* could be used as an efficient and
453 economical adsorbent for removal several dyes and some metal ions from industrial
454 wastewater.

455 **Acknowledgements**

456 This study was financially supported by the Science and Technology Supportive Project of
457 Sichuan Province, China (NO.2013SZ0062), Science and Technology Supportive Project of
458 Chengdu (No.12DXYB087JH-005) and NSFC (NO.J1103518). The authors wish to thank
459 Professor Guanglei Cheng and Dong Yu from Sichuan University for their technical assistance.

460 **References**

461 1. Akar, S.T., Gorgulu, A., Kaynak, Z., Anilan, B., Akar, T. 2009. *Chemical Engineering Journal*, 148,
462 26.
463 2. Aksu, Z., Gönen, F. 2004.. *Process Biochemistry* 39, 599.
464 3. Anandkumar, J., Mandal, B. 2011.. *J Hazard Mater* 186, 1088.
465 4. Arica, M.Y., Bayramoglu, G. 2007. *J Hazard Mater* 149, 499.
466 5. Auta, M., Hameed, B.H. 2014.. *Chemical Engineering Journal* 237, 352.
467 6. Bouzid, S., Khenifi, A., Bennabou, K.A., Trujillano, R., Vicente, M.A., Derriche, Z. 2015. *Chemical*
468 *Engineering Communications* 202, 520.
469 7. Charumathi, D., Das, N. 2012. *Desalination* 285, 22.
470 8. Das, S.K., Ghosh, P., Ghosh, I., Guha, A.K. 2008.. *Colloids Surf B Biointerfaces* 65, 30.
471 9. Dawood, S., Sen, T.K. 2012. *Water Res* 46, 1933.
472 10. Elkady, M.F., Ibrahim, A.M., Abd El-Latif, M.M. 2011. *Desalination* 278, 412.
473 11. Fu, Y.Z., Viraraghavan, T. 2002. *Bioresource Technology* 82(2), 139.
474 12. Gupta, V.K., Gupta, B., Rastogi, A., Agarwal, S., Nayak, A. 2011. *J Hazard Mater* 186, 891.
475 13. Inbaraj, B.S., Chien, J.T., Ho, G.H., Yang, J., Chen, B.H. 2006. *Biochemical Engineering Journal*
476 31, 204.
477 14. Kadirvelu, K., Karthika, C., Vennilamani, N., Pattabhi, S. 2005. *Chemosphere* 60, 1009.
478 15. Kousha, M., Daneshvar, E., Sohrabi, M.S., Jokar, M., Bhatnagar, A. 2012. *Chemical Engineering*
479 *Journal* 192, 67.
480 16. Koyuncu, H., Yildiz, N., Salgin, U., Koroglu, F., Calimli, A. 2011. *J Hazard Mater* 185, 1332.
481 17. Lei, D.-Y., Li, B., Wang, Q., Wu, B., Ma, L., Xu, H. 2014. *Desalination and Water Treatment*, 1.
482 18. Long, Y.C., Lei, D.Y., Ni, J.X., Ren, Z.L., Chen, C., Xu, H. 2014. *Bioresource Technology* 152,

457.
19. Mahmoud, D.K., Salleh, M.A.M., Karim, W.A.W.A., Idris, A., Abidin, Z.Z. 2012. *Chemical Engineering Journal* 181-182, 449.
20. Malkoc, E., Nuhoglu, Y., Abali, Y. 2006. *Chemical Engineering Journal* 119, 61.
21. Maurya, N.S., Mittal, A.K., Cornel, P., Rother, E. 2006. *Bioresour Technol* 97, 512.
22. Nguyen, T.A., Juang, R.-S. 2013. *Chemical Engineering Journal* 219, 109.
23. Noreen, S., Bhatti, H.N., Nausheen, S., Sadaf, S., Ashfaq, M. 2013.*Industrial Crops and Products* 50, 568.
24. O'Mahony, T., Guibal, E., Tobin, J.M. 2002. *Enzyme and Microbial Technology* 31, 456.
25. Ozmen, E.Y., Erdemir, S., Yilmaz, M., Bahadir, M. 2007. *Clean-Soil Air Water* 35, 612.
26. Quintelas, C., Pereira, R., Kaplan, E., Tavares, T. 2013. *Bioresour Technol* 142, 368.
27. Sadaf, S., Bhatti, H.N. 2013. *Clean Technologies and Environmental Policy* 16, 527.
28. Sajab, M.S., Chia, C.H., Zakaria, S., Sillanpää, M. 2014. *Desalination and Water Treatment*, 1.
29. Sarma, G.K., SenGupta, S., Bhattacharyya, K.G. 2011. *Separation Science and Technology* 46, 1602.
30. Singh, A., Kumar, D., Gaur, J.P. 2012. *Water Res* 46, 779.
31. Thomas, H.C. 1948. *Annals of the New York Academy of Sciences* 49, 161.
32. Tian, X.L., Li, C., Yang, H.J., Ye, Z.X., Xu, H. 2011. *Desalination and Water Treatment* 27, 319.
33. Vimala, R., Charumathi D., Das Nilanjana. 2011. *Desalination*, 275, 291.
34. Vieira, M.L.G., Esquerdo, V.M., Nobre, L.R., Dotto, G.L., Pinto, L.A.A. 2014. *Journal of Industrial and Engineering Chemistry* 20, 3387.
35. Wang, J., Guo, L., Zhang, K., Wu, Q., Lin, J. 2008. *Bioresour Technol* 99, 8524.
36. Wang L, Zhang J, Zhao R, Li C, Zhang C. 2010. *Desalination*, 254, 68.
37. Won, S.W., Choi, S.B., Chung, B.W., Park, D., Park, J.M., Yun, Y.S. 2004. *Industrial & Engineering Chemistry Research* 43, 7865.
38. Yaghmaeian, K., Moussavi, G., Alahabadi, A. 2014. *Chemical Engineering Journal* 236, 538.
39. Zhang, W., Li, H., Kan, X., Dong, L., Yan, H., Jiang, Z., Yang, H., Li, A., Cheng, R. 2012. *Bioresour Technol* 117, 40.
40. Zhou, L., Jin, J., Liu, Z., Liang, X., Shang, C. 2011. *J Hazard Mater* 185, 1045.

513 **Figure legends**

514 **Fig.1.** Effect of various modifiers on RB adsorption.

515 **Fig.2.** The morphological structure of *V. volvacea* powder before (a) and after (b) modification.

516 **Fig.3.** The FTIR of *V. volvacea* powder before and after modification.

517 **Fig.4.** Effect of biosorbent dosage on the biosorption of RB on HMV (temperature = 30℃, C_0 =

518 100 mg L^{-1}, staking speed = 145 rpm).

519 **Fig.5.** Effect of solution pH on the biosorption of RB on HMV (temperature = 30℃, C_0 = 100 mg

520 L^{-1}, staking speed = 145 rpm).

521 **Fig.6.** Effect of contact time on the biosorption of RB on HMV (temperature = 30℃, C_0 : 50-250

522 mg L^{-1}, staking speed = 145 rpm)

523 **Fig.7.** Effect of initial concentration on the biosorption of RB on HMV (temperature = 30℃,

524 staking speed = 145 rpm).

525 **Fig.8.** Isotherm plots for RB adsorption on HMV at 30℃.

526 **Fig.9.** Effect of initial RB concentration on breakthrough curves (flow rate: 2.0 mL min^{-1}, bed

527 height: 4.0 cm, pH 5).

528 **Fig.10.** Effect of flow rate on breakthrough curves (initial RB concentration: 100 mg L^{-1}, bed

529 height: 4.0 cm, pH 5).

530 **Fig.11.** Effect of bed height on breakthrough curves (flow rate: 2.0 mL min^{-1}, initial RB

531 concentration: 100 mg L^{-1}, pH 5).

532

533 **Table 1**

534 Model equations used for the prediction of the breakthrough curve.

Model	Equation	Symbols representation
Bohart-Adams	$\ln\left(\frac{C_t}{C_0}\right) = k_{BA}\,C_0 t - k_{BA}N_0(\frac{Z}{v})$	Where C_t, C_0, k_{BA}, N_0, v, Z were effluent concentration, influent concentration, kinetic constant (L mg^{-1} h^{-1}), saturation concentration (mg L^{-1}), linear flow velocity (cm h^{-1}), bed height (cm), respectively.
Thomas	$\ln(\frac{C_0}{C_t} - 1) = \frac{k_T q_0 m}{F} - k_T C_0 t$	Where k_T, q_0, F were rate constant (L mg^{-1} h^{-1}), adsorption capacity (mg g^{-1}), flow rate (L h^{-1}), respectively.
Yoon-Nelson	$\ln(\frac{C_t}{C_0 - C_t}) = k_Y t - \tau k_Y$	Where k_Y is the rate constant (h^{-1}) and τ is the time required for 50% adsorbate breakthrough (h).

535

536 Table 2

537 Model equations of adsorption isotherms studies.

Model	Equation	Symbols representation
Langmuir	$\frac{C_e}{q_e} = \frac{C_e}{q_m} + \frac{1}{q_m k_L}$	Where q_e, q_m were the corresponding adsorption capacity and maximum adsorption capacity (mg/g), respectively, C_e is the concentration of RB solution at equilibrium (mg/L), k_L is the Langmuir constant (L/mg).
Freundlich	$\ln q_e = \ln k_F + \frac{1}{n} \ln C_e$	Where k_F (L/g) and n are the Freundlich constants which indicates the adsorption capacity and adsorption intensity, respectively.
Temkin	$q_e = B \ln(AC_e)$	Where A is the Temkin isotherm energy constant (L/g) and B is the Temkin constant.

538 Table 3

539 Langmuir, Freundlich and Temkin isotherm models parameters for RB biosorption by HMV.

540

Isotherms	Parameters	293K	303K	313K
Langmuir	q_m (mg/g)	61.35	68.49	94.34
	K_L (L/mg)	0.00898	0.0118	0.00815
	R^2	0.9978	0.9983	0.9907
Freundlich	k_F (L/g)	0.862	1.226	1.132
	n	0.785	0.744	0.796
	R^2	0.9860	0.9781	0.9745
Temkin	A (L/g)	0.194	0.221	0.216
	B	9.293	10.529	12.554
	R^2	0.9295	0.9294	0.9174

541

542

543 Table 4

544 Kinetic models parameters for RB biosorption by HMV at 30℃.

545

C_0	$q_{e,exp}$	Pseudo-first-order model			Pseudo-second-order model		
(mg/L)	(mg/g)	$k_1(min^{-1})$	$q_{e1,cal}$(mg/g)	R^2	k_2(g/mg min)	$q_{e2,cal}$(mg g^{-1})	R^2
50	24.20	0.0010	13.56	0.9745	0.0085	19.24	0.9999
100	33.51	0.0046	21.82	0.9741	0.0059	25.64	0.9999
150	38.17	0.0058	26.98	0.9392	0.0019	32.67	0.9993
200	43.61	0.0067	35.01	0.9856	0.00049	43.64	0.9922
250	46.87	0.0066	39.19	0.9903	0.00031	44.89	0.9992

546

547

548 Table 5

549 Thermodynamic properties of RB biosorption on HMV.

550

Biosorbent	ΔH	ΔS	ΔG (kJ/mol)		
	(kJ/mol)	(kJ/mol)	293K	303K	313K
HMV	19.74	0.069	-0.46	-1.20	-1.84

551

552

553

554

555

556

Table 6

Parameters obtained from breakthrough curves of the fixed bed column for RB adsorption.

F (mL/min)	H (cm)	C_0 (mg/L)	t_b (min)	q_b (mg/g)	t_s (min)	q_s (mg/g)
2	4	100	54	8.08	160	21.39
2	4	50	85	8.08	282	18.27
2	4	150	40	11.83	145	27.94
2	2	100	11	3.61	106	23.86
2	6	100	72	7.98	175	16.93
3.5	4	100	31	5.80	160	19.15
0.5	4	100	83	16.15	195	27.87

Notations: F, flow rate; H, bed height; t_b, t_s were the time at breakthrough and saturation point, respectively; q_b, q_s were the adsorption capacity at breakthrough and saturation time, respectively.

Table 7

Bohart-Adams, Thomas and Yoon-Nelson models parameters of RB adsorption by HMV-packed column.

Conditions			Bohart-Adams			Thomas			Yoon-Nelson		
F	H	C_0	k_{BA}	N_0	R^2	k_T	q_0	R^2	k_Y	t	R^2
2	4	100	0.0255	2573.56	0.9817	0.0334	21.42	0.9928	3.288	1.51	0.9928
2	4	50	0.0365	2217.06	0.9898	0.0361	18.41	0.9928	1.804	3.37	0.9928
2	4	150	0.0173	4518.29	0.9779	0.0221	28.09	0.9917	3.314	1.02	0.9917
2	2	100	0.0277	3743.38	0.9738	0.0361	24.12	0.9916	4.020	0.85	0.9916
2	6	100	0.0249	2573.56	0.9897	0.0311	17.01	0.9954	3.041	2.11	0.9954
3.5	4	100	0.0372	2762.03	0.9763	0.0469	19.35	0.9924	4.689	0.92	0.9924
0.5	4	100	0.0100	4099.32	0.9913	0.0078	28.00	0.9974	1.166	5.98	0.9974

Units: F: mL min^{-1}; H: cm; C_0: mg L^{-1}; K_{BA}: L $mg^{-1}h^{-1}$; N_0: mg L^{-1}; K_T: L mg^{-1} h^{-1}; q_0: mg g^{-1}; K_Y: h^{-1}; τ: h.

570 Table 8

571 Thomas model parameters of simulated industrial wastewater treatment by HMV-packed column
572 at a flow rate of 2 mL min^{-1}.

573

Adsorbates	k_T (L mg^{-1} h^{-1})	q_0 (mg g^{-1})	R^2
NR	0.0900	11.65	0.9675
CV	0.0492	8.21	0.9758
MG	0.0647	10.29	0.9537
RB	0.0507	11.37	0.9878

574

575

576

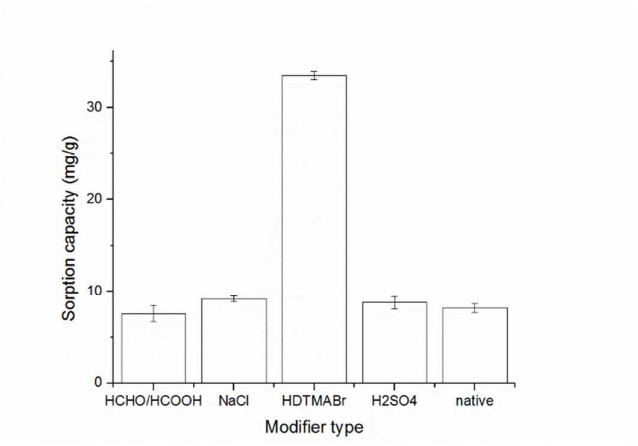

577

578 **Fig.1.** Effect of various modifiers on RB adsorption.

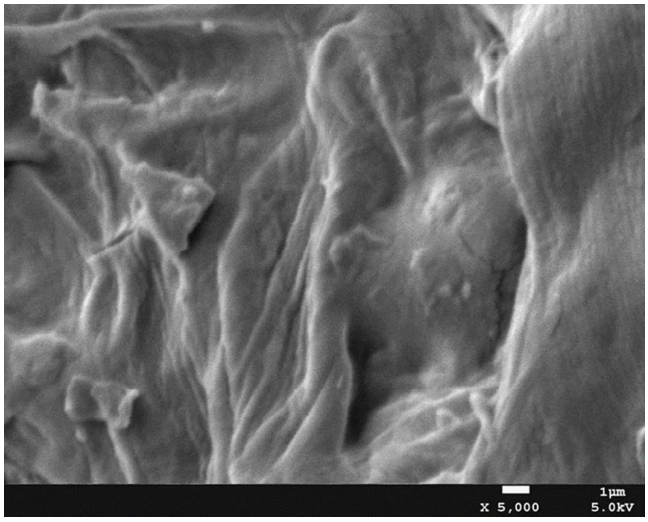

(a)

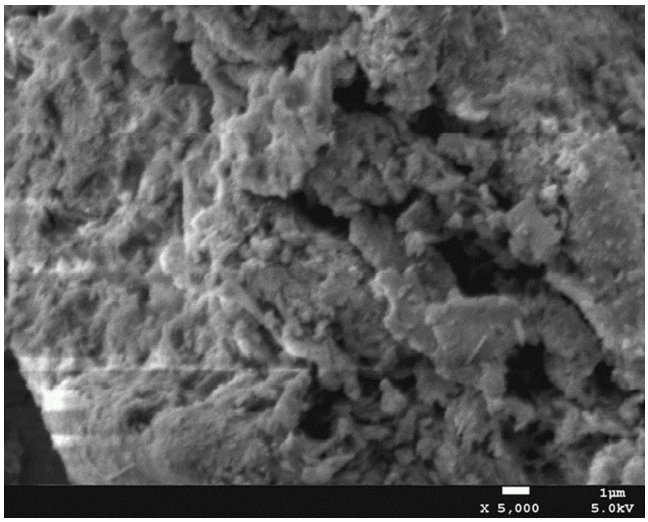

(b)

Fig.2. The morphological structure of *V. volvacea* powder before (a) and after (b) modification.

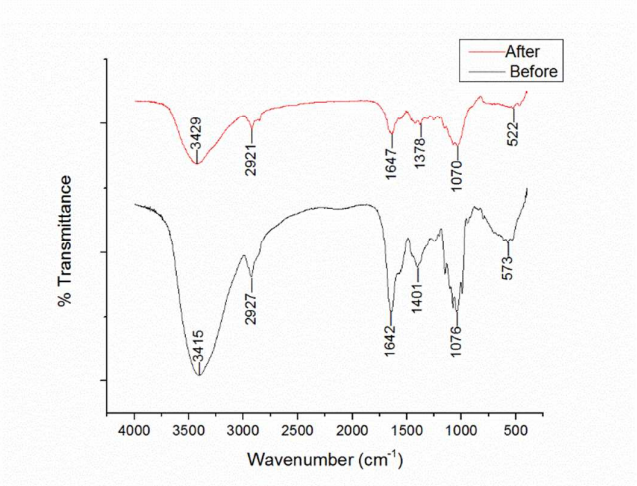

Fig.3. The FTIR of *V. volvacea* powder before and after modification.

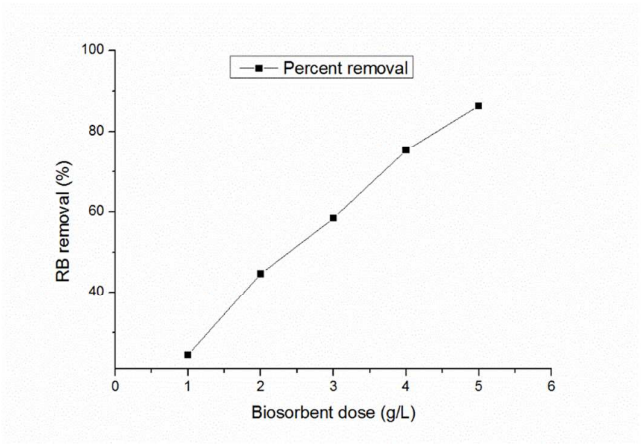

589

590 **Fig.4.** Effect of biosorbent dosage on the biosorption of RB on HMV (temperature = 30℃, C_0 =

591 100 mg L^{-1}, staking speed = 145 rpm).

592

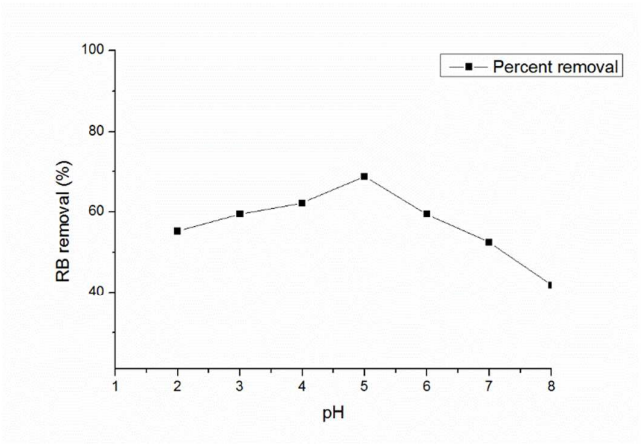

Fig.5. Effect of solution pH on the biosorption of RB on HMV (temperature = 30℃, C_0 = 100 mg L^{-1}, staking speed = 145 rpm).

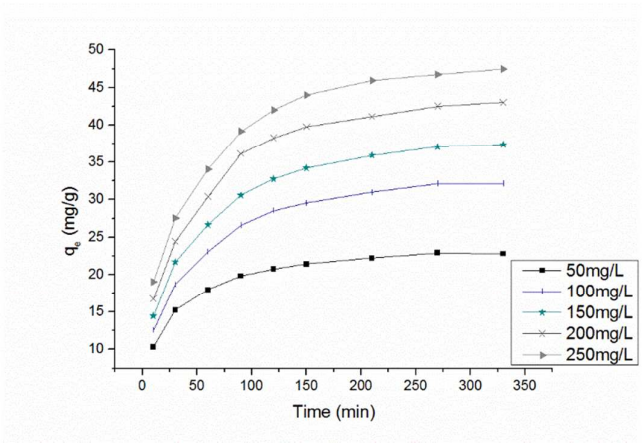

597

598 **Fig.6.** Effect of contact time on the biosorption of RB on HMV (temperature = 30℃, C_0 : 50-250

599 mg L^{-1}, staking speed = 145 rpm)

600

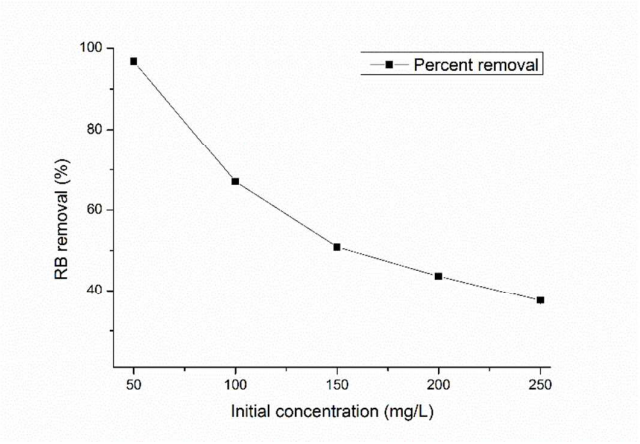

601

602 **Fig.7.** Effect of initial concentration on the biosorption of RB on HMV (temperature = 30℃,

603 staking speed = 145 rpm).

604

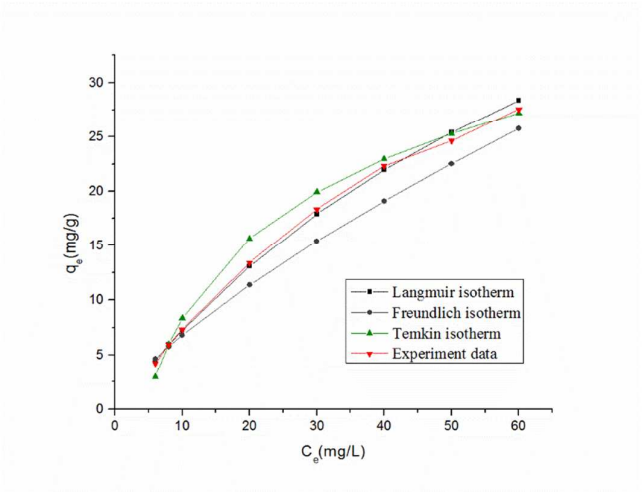

605

606 **Fig.8.** Isotherm plots for RB adsorption on HMV at 30℃.

607

608

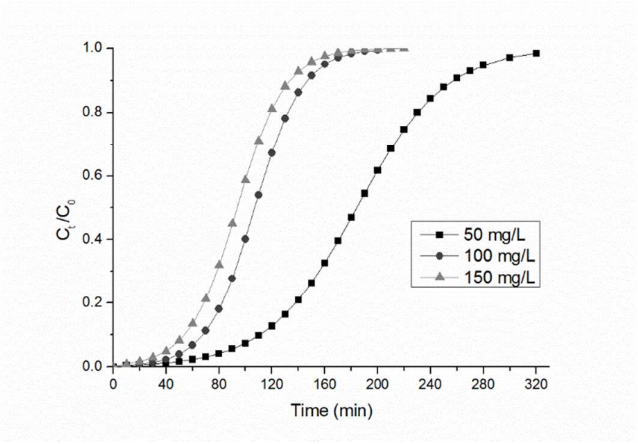

609 **Fig.9.** Effect of initial RB concentration on breakthrough curves (flow rate: 2.0 mL min^{-1}, bed

610 height: 4.0 cm, pH 5).

611

612

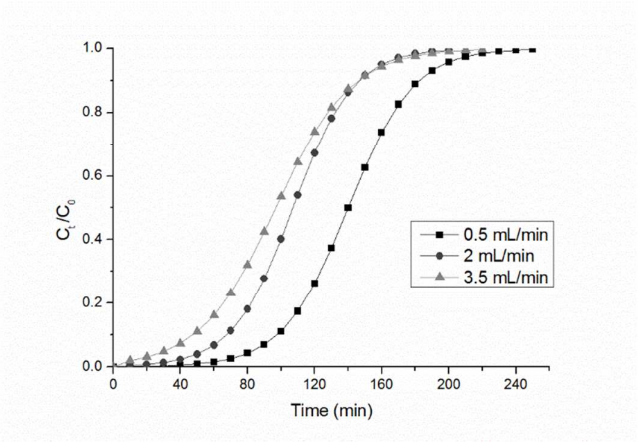

613 **Fig.10.** Effect of flow rate on breakthrough curves (initial RB concentration: 100 mg L^{-1}, bed

614 height: 4.0 cm, pH 5).

615

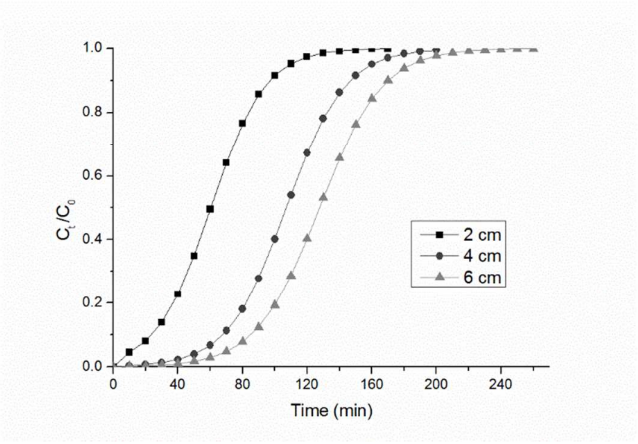

616

617 **Fig.11.** Effect of bed height on breakthrough curves (flow rate: 2.0 mL min^{-1}, initial RB

618 concentration: 100 mg L^{-1}, pH 5).

619

620